1521-0111/100/1/32–45$35.00
MOLECULAR PHARMACOLOGY

https://doi.org/10.1124/molpharm.120.000223
100:32–45, July 2021

Drug-Drug Interaction between Metformin and Sorafenib Alters Antitumor Effect in Hepatocellular Carcinoma Cells[S]

Rania Harati, Marc Vandamme, Benoit Blanchet, Christophe Bardin, Françoise Praz, Rifat Akram Hamoudi, and Christèle Desbois-Mouthon

Department of Pharmacy Practice and Pharmacotherapeutics, College of Pharmacy (R.H.), and Department of Clinical Sciences, College of Medicine (R.A.H), University of Sharjah, Sharjah, United Arab Emirates; Centre de Recherche Saint-Antoine (R.H., M.V., F.P., C.D.-M.) and Centre de Recherche des Cordeliers (C.D.-M.), Sorbonne Université, Institut National de la Santé et de la Recherche Médicale (INSERM), Université de Paris, Paris, France; Département de Pharmacocinétique et Pharmacochimie, Hôpital Cochin, AP-HP, CARPEM, Paris, France (B.B., C.B.); UMR8038 CNRS, U1268 INSERM, Faculté de Pharmacie, Université de Paris, PRES Sorbonne Paris Cité, Paris, France (B.B); Centre National de la Recherche Scientifique, Paris, France (F.P.); and Division of Surgery and Interventional Science, UCL, London, United Kingdom (R.A.H.)

Received December 17, 2020; accepted April 9, 2021

ABSTRACT

Hepatocellular carcinoma (HCC) is the most common primary liver malignancy and is one of the leading causes of cancer-related deaths worldwide. The multitarget inhibitor sorafenib is a first-line treatment of patients with advanced unresectable HCC. Recent clinical studies have evidenced that patients treated with sorafenib together with the antidiabetic drug metformin have a survival disadvantage compared with patients receiving sorafenib only. Here, we examined whether a clinically relevant dose of metformin (50 mg/kg per day) could influence the antitumoral effects of sorafenib (15 mg/kg per day) in a subcutaneous xenograft model of human HCC growth using two different sequences of administration, i.e., concomitant versus sequential dosing regimens. We observed that the administration of metformin 6 hours prior to sorafenib was significantly less effective in inhibiting tumor growth (15.4% tumor growth inhibition) than concomitant administration of the two drugs (59.5% tumor growth inhibition). In vitro experiments confirmed that pretreatment of different human HCC cell lines with metformin reduced the effects of sorafenib on cell viability, proliferation, and signaling. Transcriptomic analysis confirmed significant differences between xenografted tumors obtained under the concomitant and the sequential dosing regimens. Taken together, these observations call into question the benefit of parallel use of metformin and sorafenib in patients with advanced HCC and diabetes, as the interaction between the two drugs could ultimately compromise patient survival.

SIGNIFICANCE STATEMENT

When drugs are administered sequentially, metformin alters the antitumor effect of sorafenib, the reference treatment for advanced hepatocellular carcinoma, in a preclinical murine xenograft model of liver cancer progression as well as in hepatic cancer cell lines. Defective activation of the AMP-activated protein kinase pathway as well as major transcriptomic changes are associated with the loss of the antitumor effect. These results echo recent clinical work reporting a poorer prognosis for patients with liver cancer who were cotreated with metformin and sorafenib.

Introduction

Primary liver cancer ranks at the sixth and fourth positions in terms of incidence and mortality, respectively, and hepatocellular carcinoma (HCC) accounts for 90% of cases (Ferlay et al., 2019). Treatment options for HCC are limited, and outcomes remain poor, especially for unresectable advanced tumors. The multitarget inhibitors sorafenib and lenvatinib have been approved as first-line treatments for patients with advanced HCC. These therapies have demonstrated significant but modest effects on overall survival (Yarchoan et al., 2019).

These last years, the etiological and epidemiologic landscape of HCC has undergone significant changes. Although chronic viral hepatitis B and C and massive alcohol

This work was supported by grants from Institut National de la Santé et de la Recherche Médicale, Cancéropôle Ile de France, Institut National du Cancer [INCa-DGOS_5790], and the University of Sharjah [Competitive Grant 1701110321-P].
The authors declare no conflict of interest.
https://doi.org/10.1124/molpharm.120.000223.

[S] This article has supplemental material available at molpharm.aspetjournals.org.

ABBREVIATIONS: ABC, ATP-binding cassette; ADAM8, ADAM metallopeptidase domain 8; AICAR, *N*1-(β-D-ribofuranosyl)-5-aminoimidazole-4-carboxamide; AKT2, AKT serine/threonine Kinase 2; AMPK, AMP-activated protein kinase; CCL20, C-C motif chemokine ligand 20; CEACAM1, carcinoembryonic antigen-related cell adhesion molecule 1; FGF2, fibroblast growth factor 2; GPCR, G-protein–coupled receptor; GSEA, gene set enrichment analysis; HCC, hepatocellular carcinoma; HPRT, hypoxanthine guanine phosphoribosyltransferase; IQR, interquartile range; IRS2, insulin receptor substrate 2; MAPK, mitogen-activated protein kinase; MTT, 3-(4,5-dimethylthiazol-2-yl)-2, 5-diphenyltetrazolium bromide; OATP, organic anion-transporting polypeptide; OCT1, organic cation transporter-1; OR, olfactory receptor; PKA, protein kinase A; PRKAR1A, protein kinase cAMP-dependent type I regulatory subunit alpha; RLIP76, Ral interacting protein of 76 kDaSLC, solute carrier; RTK, receptor tyrosine kinase; STAT3, signal transducer and activator of transcription 3; T2D, type 2 diabetes.

consumption have been the major etiological factors for decades, the worldwide epidemic of obesity and type 2 diabetes (T2D) has revealed that these metabolic diseases are involved in the pathogenesis of HCC because of their ability to induce metabolic-associated steatohepatitis. Metabolic-associated steatohepatitis is becoming the leading etiology underlying many cases of HCC, especially in industrialized countries (Anstee et al., 2019; Younossi et al., 2019).

Metformin, a widely used oral biguanide for T2D treatment, has been associated with a lower risk of HCC among patients with diabetes (Zhou et al., 2016; Cunha et al., 2020) and with increased survival among patients with HCC treated with surgery (Schulte et al., 2019). However, recent clinical studies have raised doubt about the efficacy of metformin and sorafenib administration in patients with diabetes with advanced HCC. Indeed, it has been reported that patients treated with sorafenib had a survival disadvantage when they were treated with metformin, their overall survival being 4 to 5 months shorter compared with patients receiving sorafenib only (Casadei Gardini et al., 2015, 2017; Schulte et al., 2019). Conversely, patients with HCC receiving insulin treatment showed a better response to sorafenib and longer survival (Casadei Gardini et al., 2017).

Using murine experimental models, it has been reported that the concomitant administration of metformin with sorafenib (30 mg/kg per day) was more efficient than monotherapies to inhibit growth and metastatic dissemination of orthotopically engrafted MHCC97H cells (Guo et al., 2016; You et al., 2016). The metformin and sorafenib combination also led to growth inhibition of subcutaneously xenografted Bel-7402 cells compared with single agent (Ling et al., 2017). However, it is important to note that these studies were conducted with a high dose of metformin (200 mg/kg per day), which is not consistent with the therapeutic doses achievable in patients with diabetes (33–42 mg/kg per day). In addition, drugs were administered according to a single regimen, i.e., concomitant administration. Recently, Karbownik et al. (2020) reported that the coadministration of metformin (100 mg/kg) and sorafenib (100 mg/kg) to rats increased the clearance of sorafenib, resulting in a lower half-life of sorafenib. This study points a potential pharmacokinetic interaction between metformin and sorafenib.

The present study was designed to examine whether a clinically relevant dose of metformin (50 mg/kg per day) has antitumoral effects when administered with sorafenib (15 mg/kg per day) according to two different sequences, i.e., concomitant versus sequential. These experiments were conducted in a subcutaneous xenograft model of human HCC growth as well as in a panel of human HCC cell lines.

Materials and Methods

Pharmacological Drugs. Sorafenib (*p*-Toluene sulfonate salt) was purchased from LC Laboratories (Woburn, MA), and metformin was from Sigma-Aldrich (Saint-Quentin Fallavier, France). For in vitro studies, sorafenib and metformin were dissolved in dimethylsulfoxide (Sigma-Aldrich Chemie S.a.r.l., Saint-Quentin Fallavier, France) and serum-free medium, respectively. For in vivo studies, sorafenib and metformin were dissolved in Cremophor EL/ethanol/water (12.5%:12.5%:75%, Sigma-Aldrich) and sterile water, respectively. *N*1-(β-D-ribofuranosyl)-5-aminoimidazole-4-carboxamide (AICAR) was from Tocris Bioscience (Bio-Techne Europe, Lille, France).

Xenografts. All in vivo experiments were approved by Charles Darwin Ethics Committee and French Ministry of Higher Education and Research under protocol number 01350.02.

Female athymic mice (6 weeks old; Rj:NMRI-Foxn1nu/Foxn1nu; Janvier Laboratories, Le Genest-Saint-Isle, France) were inoculated subcutaneously in the right flank with 2×10^6 PLC/PRF5 cells suspended in 50% Matrigel (BD Biosciences, San Jose, CA). Mice were treated by gavage with vehicles (control), sorafenib alone (15 mg/kg per day), metformin alone (50 mg/kg per day), metformin combined with sorafenib (concomitant schedule), and metformin followed 6 hours later by sorafenib (sequential schedule). Mice were randomly assigned to the different experimental groups. In the first set of experiments, designed to evaluate the preventing effect of metformin on tumor growth, metformin ($n = 7$) and vehicle ($n = 7$) administrations were initiated 4 days before HCC cell grafts and maintained during the next 15 days. In the second set of experiments, designed to evaluate the metformin/sorafenib combination, sample sizes were selected before any data had been obtained and were unequal. The control group was selected as the largest one ($n = 19$). The sizes of metformin, concomitant, and sequential groups were equivalent ($n = 12$–14). The sorafenib group was chosen as the smaller one ($n = 10$) as a result of low variability in tumor growth response (Blivet-Van Eggelpoel et al., 2012). Tumor size was measured three times a week using a hand caliper, and tumor volume was calculated using the formula length $\times$ (width)^2 $\times$ 0.52. Tumor volume measurements were not blinded, but were carried out by the same person. Mice were weighed three times a week to follow drug toxicity. Weight loss greater than 15% was considered a sign of toxicity. After 15 days, mice were anesthetized, and tumors were excised, weighed, flash frozen in liquid nitrogen, and stored at −80°C for further analyses. We observed a strong correlation between tumor volumes and weights (data not shown).

Plasma Concentrations of Metformin and Sorafenib. Plasmas were prepared from blood collected by cardiac puncture. Plasma concentrations of sorafenib were determined 2 hours and 6 hours postadministration by gavage using a previously described high-performance liquid chromatography method. The accuracy, within-assay, and between-assay precision of this method were 96.9%–104.0%, 3.4%–6.2%, and 7.6%–9.9%, respectively (Blanchet et al., 2009). Plasma concentrations of metformin were determined 2 and 4 hours postadministration by gavage using a modified ultrahigh-pressure liquid chromatography assay with UV diode array detector as previously described (Bardin et al., 2012). The calibration curve for metformin was linear within the range of 0.15–20.0 mg/l. Based on quality-control samples, the accuracy, within-assay, and between-assay precision were less than 10% of the entire range of quantification. The accuracy of our method was ensured by our participation in the metformin proficiency testing scheme provided by the Société Française de Toxicologie Analytique.

Cell Culture and Treatments. HepG2, Hep3B, and Huh7 cells were obtained from the American Type Culture Collection. PLC/PRF5 were provided by Dr. Christine Perret (Institut Cochin, France). Cell line authentication was performed by using a panel of nine short tandem repeats as previously reported (Goumard et al., 2017). Cell lines were cultured as reported elsewhere (Blivet-Van Eggelpoel et al., 2012) and routinely controlled for mycoplasma contamination. Human hepatocytes in primary culture were obtained as reported elsewhere (Aoudjehane et al., 2016).

Cell Viability and Proliferation. Cell viability was evaluated using the 3-(4,5-dimethylthiazol-2-yl)-2,5-diphenyltetrazolium bromide assay (MTT assay) as previously reported (Desbois-Mouthon et al., 2009). Cell proliferation was evaluated by direct cell counting and by staining DNA with 0.1% crystal violet in 20% methanol for 30 minutes at room temperature with gentle shaking. Crystal violet dye was extracted using 10% SDS and 0.01 mM HCl at 37°C for 1 hour, and absorbance was determined at 570 nm in a microplate reader (Infinite F200 PRO, Tecan, Switzerland).

Western Blotting. Protein electrophoresis and transfer to nitrocellulose were performed according to standard procedures, and primary antibodies against phospho-AMPKα (Thr172) (40H9) and AMPKα (Cell Signaling Technology Europe, Leiden, Netherlands) were used. Blot revelations were performed using ChemiDocTM Touch Imaging System (BIO-RAD, Hercules, CA).

RNA Isolation and Analysis of Gene Expression. Total RNA was extracted from cell cultures using Nucleospin RNA kit (Macherey-Nagel SARL, Hoerdt, France). Quantitative measurements of transcripts were performed by real-time polymerase chain reaction on a LightCycler 96 instrument (Roche Diagnostics, Meylan, France) using SYBR Green chemistry and specific primers for *ABCB1* (*ATP binding cassette subfamily B member 1* coding for MDR1 (multidrug resistance-1)/PgP (P-glycoprotein 1)) (forward: 5′-GAAATTTAGAAGATCTGATGT-CAAACA-3′, reverse: 5′-ACTGTAATAATAGGCATACCTGGTCA-3′), *ABCG2* (coding for BCRP (breast cancer resistance protein)) (forward: 5′-TGGCTTAGACTCAAGCACAGC-3′, reverse: 5′-TCGTCCCTGCTTA-GACATCC-3′), *RALBP1* (*RalA binding protein 1*) (coding for RLIP76 (Ral interacting protein of 76 kDa)) (forward: 5′-CGGCTCTCTCGCT GTACATT-3′, reverse: 5′-GAACCTGAGCCTGACGTGAA-3′), *SLC22A1* (*solute carrier family 22 Member 1*) (coding for organic cation transporter-1 (OCT1)) (forward: 5′-CTGAGGGAGACATTGCACCT-3′, reverse: 5′-TGCTCCAGAATGTCATCCAC-3′), *SLCO1B1* (coding for OATP1B1) (forward: 5′-GGGTGGACTTGTTGCAGTTG-3′, reverse: 5′-TGTTTTT GTTGTTGATGCTCAGT-3′), and *SLCO1B3* (coding for OATP1B3) (forward: 5′-TCAAGTGGTATTAAAAAGCATACAGTG-3′, reverse: 5′- TTC ACCCAAGTGTGCTGAGT-3′). For each sample, gene expression was normalized to that of *hypoxanthine guanine phosphoribosyltransferase (HPRT)* mRNA content (forward: 5′-TAATTGGTGGAGATGATCT-3′, reverse: 5′-TGCCTGACCAAGGAAAGC-3′). *HPRT* mRNA was used to standardize reverse transcription-quantitative polymerase chain reaction experiments because this transcript is one of the most stable house-keeping mRNAs between the different HCC cell lines, and its Cq values were close to those of the genes of interest. In addition, the expression of HPRT mRNA was not altered after metformin treatment in HCC cell lines (data not shown). The relative quantity of each target gene was determined from replicate samples using the formula $2^{-\Delta\Delta Ct}$.

Uptake of Radiolabeled Sorafenib. HCC cells (7×10^4 cells per well) grown in 24-well plates were preincubated for 30 minutes at 37°C in uptake buffer (96 mM NaCl, 5.3 mM KCl, 1.1 mM $KH2PO_4$, 0.8 mM $MgSO_4$, 1.8 mM $CaCl_2$, 11 mM D-glucose, 50 mM HEPES, pH 7.4). Experiments were initiated by replacement of uptake medium with 0.5 ml of 0.2 μCi/mL [^{3}H]sorafenib [0.1–3 Ci (3.7–111 GBq)/mmol; Moravek Inc., Brea, CA] in uptake buffer. Initially, time-dependent experiments were conducted for up to 20 minutes to determine the linear uptake range (unpublished data). After incubation, radioactive solutions were aspirated, and cells were washed four times with 4°C uptake buffer. Cells were lysed with 500 μL of 0.1 N NaOH/0.1% SDS for 4 hours, and samples were analyzed by liquid scintillation counting. Data were normalized to protein concentration determined using bicinchoninic acid protein assay reagent kit.

Gene Expression Microarray. Total RNA was extracted using Trizol (Thermo Fisher Scientific) from tumors collected from mice xenografted and treated with vehicle (control), metformin (50 mg/kg per day) combined with sorafenib (15 mg/kg per day) (concomitant schedule), or metformin (50 mg/kg per day) followed 6 hours later by sorafenib (15 mg/kg per day) (sequential schedule). RNA integrity was assessed using the Agilent 2100 Bioanalyzer (Agilent Technologies, Palo Alto, CA). Total RNA was amplified and labeled using the GeneChip WT PLUS Reagent Kit (Thermo Fisher Scientific). Each RNA sample was hybridized to Human Clariom S GeneChip (Thermo Fisher Scientific). Arrays were scanned, and images were analyzed and controlled for hybridization artifacts.

Microarray Analysis. The microarray data were normalized using Signal Space Transformation-RMA, which is optimized for underestimation of true fold changes (Irizarry et al., 2003). After normalization, differential expression was carried out using eBayes function and one-way ANOVA statistical analysis. The analysis was carried out using Transcriptome Analysis Console software (Thermo Fisher Scientific, version 4.0.2), with $P < 0.05$ considered as statistically significant. The differentially expressed genes were then subjected to absolute gene set enrichment analysis (GSEA) searching through more than 10,000 different cellular pathways as described in Hamoudi et al. (2010). C2 is a collection in The Molecular Signature Database consisting of sets curated from biomedical literature and online pathway databases such as the Kyoto Encyclopedia of Genes and Genome (Kanehisa and Goto, 2000) or Reactome (Croft et al., 2011). The gene ontology set C5 contains curated sets derived from Gene Ontology (Ashburner et al., 2000). The data discussed in this publication have been deposited in National Center for Biotechnology Information's Gene Expression Omnibus (GEO) and are accessible through GEO series accession number GSE162557.

Statistical Analysis. The experiments performed in this study were exploratory in nature and designed to evaluate the antitumoral effects of metformin in combination with sorafenib according to two different regimens. The current study did not employ a predefined study design; as such, reported *P* values are descriptive. Statistical analyses were performed using GraphPad Prism software (San Diego, CA). When a parametric distribution was assumed, data are provided as means ± S.D. and statistically analyzed with one-way ANOVA (post hoc Tukey's test). When a nonparametric distribution was assumed, data are presented as medians (IQR) and statistically analyzed with Kruskal-Wallis test (post hoc Dunn's test). Differences were considered statistically significant at $P < 0.05$.

Results

In Vivo Effects of a Clinically Relevant Dose of Metformin in Combination with Sorafenib on HCC Growth

A low dose of metformin (50 mg/kg per day) was administered by gavage in the following experiments. This dose, which is comparable with that used in metformin-treated patients with diabetes (33.3–42.5 mg/kg per day), has been reported to reduce insulin resistance and to normalize blood glucose levels in diabetic mice but had no effect on glycemia in control mice (Heishi et al., 2006; Foretz et al., 2010; Hou et al., 2010). We confirmed that the intragastric administration of 50 mg/kg per day metformin to nude mice led to median (IQR) plasma metformin concentrations that reached 0.56 (0.36–0.73) mg/l 2 hours after administration (Table 1), which was close to the therapeutic values observed in humans (Lalau et al., 2011).

The first set of experiments was designed to evaluate the effect of the low dose of metformin alone on tumor growth in a model of subcutaneously xenografted PLC/PRF5 cells. Metformin and vehicle administrations were initiated 4 days before HCC cell grafts and maintained during the next 15 days. We observed that 50 mg/kg per day metformin altered neither tumor initiation (100% of mice developed tumors) nor the kinetics of tumor growth in comparison with the control group (Fig. 1, A and B).

In the second set of experiments, the ability of 50 mg/kg per day metformin to improve the antitumoral effect of sorafenib was evaluated on established xenografted tumors (~250 mm^3). A dose of 15 mg/kg per day sorafenib was used in these experiments, which is equivalent to that used in humans for the treatment of advanced HCC (800 mg/day). This dose led to median (IQR) plasma sorafenib concentrations of 2.98 (1.34–3.23) mg/l 2 hours postadministration in nude mice (Table 1) (therapeutic concentrations in humans: 2–5 mg/l). To define the optimal sequence, two administration schedules were followed: metformin was administered concomitantly with sorafenib

TABLE 1
Plasma concentrations of metformin and sorafenib. Values are medians (IQR); significances between sorafenib, concomitant, and sequential groups were tested using Kruskal-Wallis test.

	Metformin		Sorafenib	
	2 h	4 h	2 h	6 h
	mg/l			
Monotherapy (n = 3)	0.56 (0.36–0.73)	0.22 (0.18–0.49)	2.98 (1.34–3.23)	0.61 (0.61–0.77)
Concomitant (n = 4)			2.04 (1.84–3.08)	1.06 (0.63–1.38)
Sequential[a] (n = 4)			2.07 (1.68–5.22)	
Sequential[b] (n = 3)			3.16 (2.03–5.20)	

[a]Metformin was administered 2 h before sorafenib.
[b]Metformin was administered 4 h before sorafenib.

(concomitant schedule) or 6 hours before sorafenib (sequential schedule). In mice, the plasma half-life of metformin is relatively short (1 to 2 hours), and metformin concentrations in xenografted tumors have also been reported to decrease rapidly (Dowling et al., 2016; Cai et al., 2019). Thus, we chose a 6-hour interval between the two drugs to administer sorafenib when intratumoral concentrations of metformin were supposed to be low. Groups of mice receiving vehicle, sorafenib, or metformin alone were run in parallel. Of note, four mice in the concomitant group showed signs of tumor necrosis in the course of the experiment, which led to sacrifice and excluding them from analysis. As shown on Fig. 1, C and D and Table 2, 15 mg/kg per day sorafenib alone significantly reduced tumor volume by 42.3% as compared with the control group. When metformin and sorafenib were administered concomitantly, tumor volumes were significantly reduced and tended to be smaller than those obtained with sorafenib alone (59.5% tumor growth inhibition as compared with the control group). In contrast, the sequential therapy had no significant antitumor effect (15.4% tumor growth inhibition as compared with the control group). The analysis of tumor weights at sacrifice confirmed that the sequential schedule was not effective to reduce tumor weight (Fig. 1E). None of the different treatments showed toxicity as monitored by body weight evaluation (data not shown). Altogether, these data indicate that metformin has schedule-dependent antitumor effects against HCC cells when combined with sorafenib; the sequential schedule (administration of metformin 6 hours before sorafenib) seems to impair the anticancer activity of sorafenib.

Effects of Metformin on Plasma Concentrations of Sorafenib

To approach the potential mechanisms accounting for metformin-mediated inhibition of sorafenib effect, we first measured plasma concentrations of sorafenib. The maximal plasmatic concentrations of sorafenib in mice have been previously reported between 1.5 and 2 hours after oral administration (https://www.ema.europa.eu/en/documents/scientific-discussion/nexavar-epar-scientific-discussion_en.pdf; Edginton et al., 2016). Therefore, sampling points performed 2 and 6 hours after sorafenib administration were chosen to characterize the absorption and elimination phases of sorafenib pharmacokinetics, respectively. Plasma concentrations were measured in mice treated with sorafenib alone, sorafenib and metformin concomitantly for 2 or 6 hours, as well as in mice pretreated with metformin for 2 or 4 hours and then exposed to sorafenib for 2 hours. As shown in Table 1, the concomitant and sequential administrations of metformin did not modify the plasmatic concentrations of sorafenib as compared with those obtained in mice treated with sorafenib alone.

TABLE 2
Tumor growth inhibition rates

	TGI[a] (Day 15) %
Control (n = 19)	
Metformin (n = 14)	11.7
Sorafenib (n = 10)	42.3
Concomitant (n = 8)	59.5
Sequential (n = 14)	15.4

[a]Tumor growth inhibition (TGI) rates were calculated using the formula (1 − TVt/TVc)*100, where TVt and TVc are the mean tumor volumes of treated and control groups, respectively.

In Vitro Effects of Metformin in Combination with Sorafenib on HCC Cell Viability and Proliferation. We then analyzed the effects of metformin and sorafenib on the viability of the PLC/PRF5 cell line using an in vitro MTT assay. As shown in Fig. 2, A and B, the concomitant treatment of PLC/PRF5 cells with suboptimal concentrations of metformin and sorafenib decreased cell viability to a larger extent than did each drug alone. In contrast, the sequential treatment (pretreatment with metformin for 6 hours) was significantly less effective to reduce cellular viability than the concomitant treatment. We extended analyses to three other human liver cancer cell lines—namely, Hep3B, HepG2, and Huh7. In these three cell lines, the concomitant combination of metformin with sorafenib was significantly more efficient to reduce cell viability than was the sequential schedule (Fig. 2A).

As metformin is known to affect the mitochondrial complex 1 of the respiratory chain, it might interfere with the MTT assay, which relies on mitochondrial activity. Therefore, we also evaluated the effects of concomitant and sequential treatments on HCC cell proliferation using two assays that do not rely on cell functionalities. As shown in Fig. 3, A and B, the concomitant treatment was more potent than the sequential schedule to reduce proliferation in PLC/PRF5 and Huh7 cells evaluated both by cell counting and DNA staining with crystal violet. Altogether, these data support the conclusion that when metformin was administered before, the antiproliferative effect of sorafenib was reduced in vitro.

Effects of Metformin on Sorafenib Uptake in HCC Cells

We then investigated whether metformin may alter sorafenib uptake in HCC cells. Sorafenib uptake has been reported to occur via both passive (Hu et al., 2009; Swift et al., 2013)

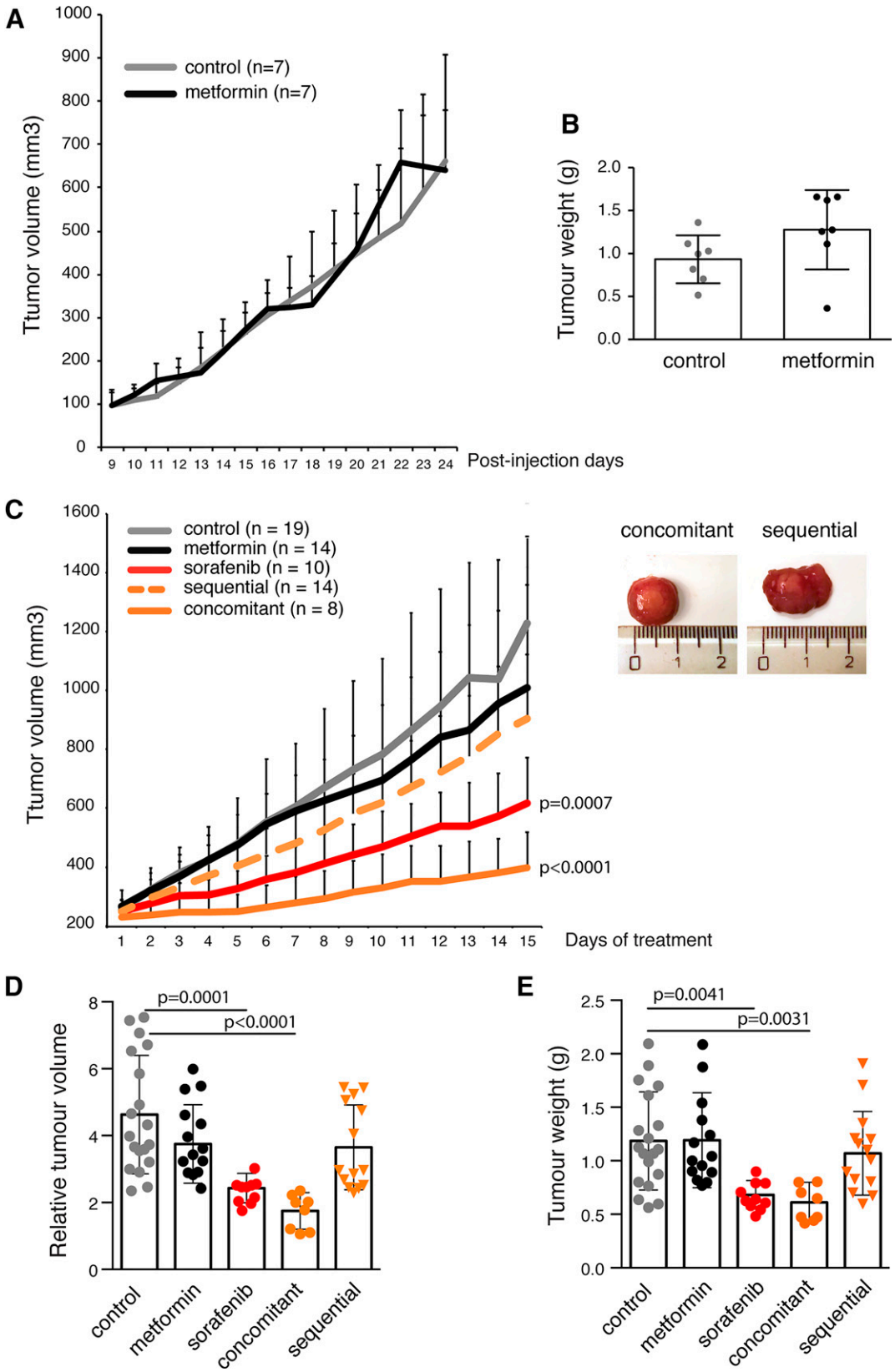

Fig 1. Effects of the concomitant and sequential combinations of metformin and sorafenib on tumor growth in an HCC xenograft model. (A) Low doses of metformin (50 mg/kg per day, $n = 7$) and vehicle ($n = 7$) were administered to 6-week-old athymic mice 4 days before subcutaneous xenografts with 2×10^6 PLC/PRF5 cells and maintained during the next 15 days. The evolution of tumor volumes over the 15 days of treatment is presented. (B) Tumor weights at sacrifice. (C) The 6-week-old athymic mice were inoculated subcutaneously with 2×10^6 PLC/PRF5 cells.Once tumor volumes reached 250 mm^3, mice were treated by gavage with vehicles (control, $n = 19$), sorafenib alone (15 mg/kg per day, $n = 10$),

and active (Herraez et al., 2013; Swift et al., 2013; Zimmerman et al., 2013) diffusion in different cell types. The active portion may involve OATP1B1 and 1B3 and OCT1. As shown in Fig. 4A, hepatic cancer cell lines exhibited low levels of OATP1B1, OATP1B3, and OCT1 transcripts compared with normal human hepatocytes. Cell treatment with metformin (1 mM, 24 hours) had no effect on mRNA expression of influx transporters (data not shown).

Efflux clearance of sorafenib has been shown to be mediated by different transporters. BCRP/ABCG2 functions as an efflux pump for sorafenib in vivo in mouse brain (Agarwal et al., 2011; Agarwal and Elmquist, 2012; Tang et al., 2013) and in vitro in MDCKII and Hep3B cells (Poller et al., 2011; Huang et al., 2013). RLIP76, a stress-responsive membrane protein, has been identified as a transporter for sorafenib in kidney cancer cells (Singhal et al., 2010). In contrast, sorafenib seems to be a weak substrate for Pgp/MDR1/ABCB1 in vitro in the K562/Dox cell line (Haouala et al., 2010) and in vivo in mouse (Agarwal and Elmquist, 2012). These three pumps were expressed differentially in HCC cell lines (Fig. 4B), and cell treatment with metformin (1 mM, 24 hours) was without any effect on mRNA expression of efflux transporters (data not shown).

We examined whether cell pretreatment with metformin may impact drug uptake using radiolabeled [^{3}H]sorafenib. Experiments were performed at 37°C and also at 4°C to assess the contribution of passive diffusion to overall uptake. The uptake of [^{3}H]sorafenib at 4°C was reduced by 58% compared with 37°C, confirming a substantial degree of passive diffusion (Fig. 4C). At both temperatures, cell pretreatment with metformin during 6 hours did not alter sorafenib cellular accumulation (Fig. 4, C and D). These data did not support a role of metformin on the regulation of sorafenib disposal into HCC cells in vitro.

In Vitro Effects of Metformin in Combination with Sorafenib on AMPK Phosphorylation. The combination of metformin and sorafenib has been reported to be synergistic in non–small-cell lung cancer cells through AMPK activation (Groenendijk et al., 2015). Therefore, we next investigated whether sequential and concomitant regimens differentially affected the AMPK pathway. Using AICAR, which is a cell-permeable activator of AMPK (through its phosphorylation), in different cancer cell lines including HCC cells (Cheng et al., 2014), we observed that the concomitant treatment of PLC/PRF5 and Huh7 cells with AICAR and sorafenib reduced cell viability more efficiently than drugs alone, and the sequential treatment turned out to be less potent (Fig. 5A). These data mimic those obtained with the metformin/sorafenib combinations (Fig. 2) and suggest that the crossresistance observed between metformin and sorafenib in the sequential schedule may be associated with an inadequate stimulation of AMPK activity. To test this hypothesis, the phosphorylation level of AMPK was examined by Western blot analysis in the different cell lines treated for 24 hours with drugs alone, drugs in combination, or metformin for 6 hours followed by sorafenib for the next 18 hours. As shown in Fig. 5B, the concomitant treatment increased the activation level of AMPK in comparison with control, whereas the sequential treatment led to a lower activation of AMPK in the four HCC cell lines.

Genes Differentially Expressed in Concomitant and Sequential Regimens

To better characterize the molecular signatures driving the differential responses to concomitant and sequential bitherapies, we conducted a transcriptomic analysis on RNA extracted from tumor xenografts. Using ANOVA to filter differentially expressed genes obtained from eBayes function, 1035 genes were identified to be differentially expressed between control and concomitant treatments, 771 genes between control and sequential treatments, and 1051 between sequential and concomitant treatments. Among these differentially expressed genes, 193 were commonly altered by both types of treatments (sequential and concomitant), 842 genes were altered by the concomitant treatment only, and 578 genes by the sequential treatment (Fig. 6, A and B).

The differentially expressed genes were subjected to absolute GSEA searching through more than 10,000 different cellular pathways (Fig. 6B). The analysis identified 6 and 24 pathways derived from the C2 and C5 gene sets, respectively, as differentially expressed between the control and concomitant treatments, and 15 and 18 pathways derived from the C2 and C5 gene sets, respectively, were differentially expressed between the control and sequential treatments (Supplemental Tables S2 and S3). Ten pathways derived from C2 gene sets and five pathways from C5 gene sets were differentially expressed between concomitant and sequential treatments (Supplemental Table 4).

Some of the pathways identified for the concomitant treatment are related to G-protein–coupled receptors (GPCR) and transmembrane receptors signaling such as GO_G_PROTEIN_COUPLED_RECEPTOR_ACTIVITY (GO:0007186) and GO_TRANSMEMBRANE_SIGNALING_RECEPTOR_ACTIVITY (GO:0004888). Some of the pathways identified for the sequential treatment are related to protein kinases, receptor tyrosine kinases (RTKs), and mitogen-activated protein kinase (MAPK) signaling, such as REACTOME SIGNALING BY RECEPTOR TYROSINE KINASES (R-HSA-9006934), POSITIVE REGULATION OF MAPK CASCADE (GO:0043410), and GO_REGULATION_OF_PHOSPHORUS_METABOLIC_PROCESS (GO:0051174). Some of the pathways differentially expressed between sequential and concomitant treatments are also related to GPRC, such as REACTOME_SIGNALING_BY_GPCR (R-HSA-372790), REACTOME_GPCR_LIGAND_BINDING (R-HSA-500792), and GO_G_PROTEIN_COUPLED_RECEPTOR_ACTIVITY (GO:0004930), as well as cell proliferation, such as BENPORATH_EED_TARGETS (M7617) (Fig. 6C).

metformin alone (50 mg/kg per day, $n = 14$), metformin combined with sorafenib (concomitant schedule, $n = 8$), or metformin followed 6 hours later by sorafenib (sequential schedule, $n = 14$). The evolution of tumor volumes over the 15 days of treatment is presented. Inset: representative photographs of tumors at sacrifice after concomitant or sequential treatment. (D) Relative tumor volumes were calculated for each group using the formula TVd15/TVd1, where TVd15 and TVd1 are the mean tumor volumes at day 15 and day 1, respectively. (E) Tumor weights at sacrifice. Data are means ± S.D. *P* values were determined using one-way ANOVA relative to the control condition.

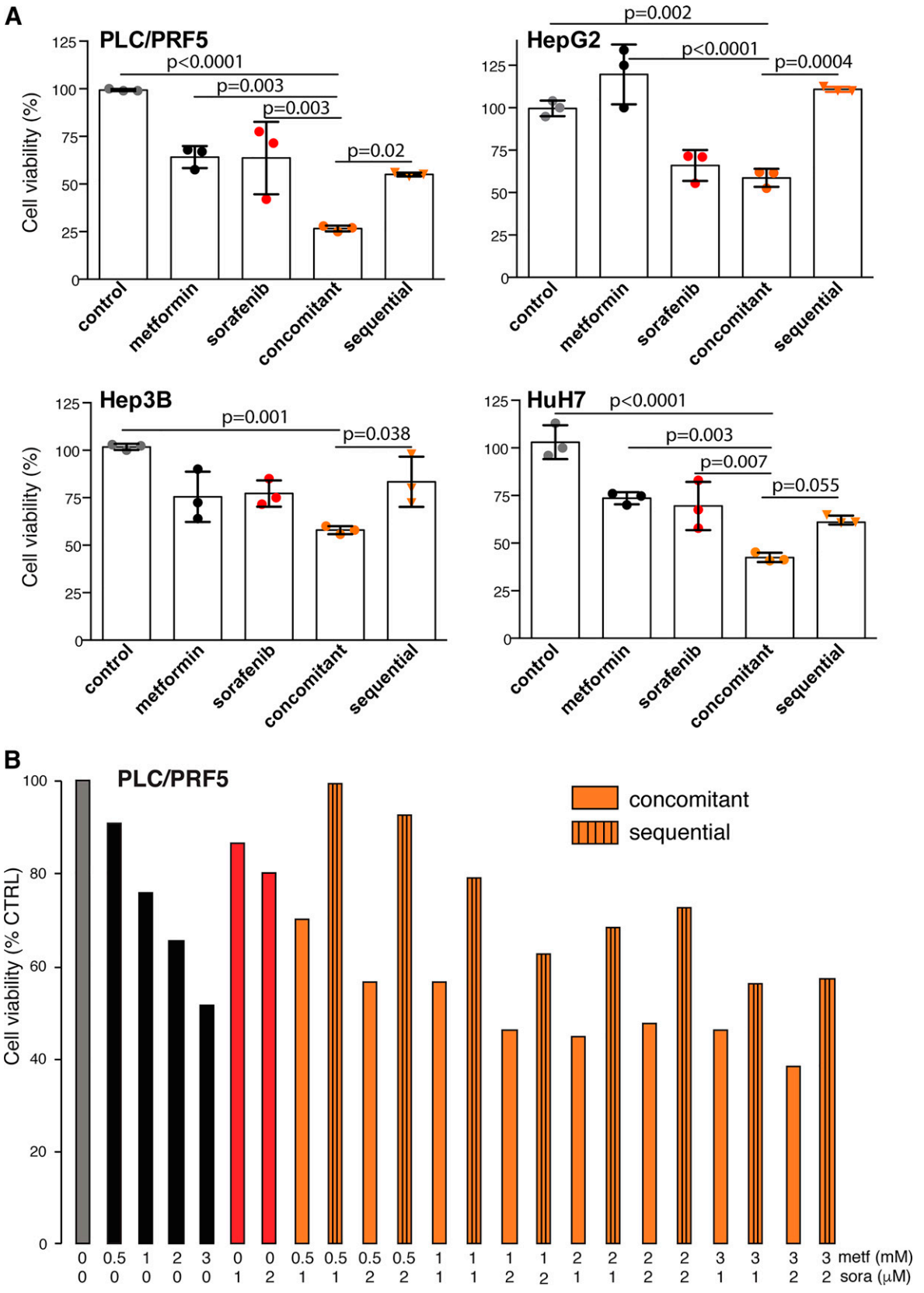

Fig 2. Effects of the concomitant and sequential combinations of metformin and sorafenib on cell viability in human HCC cell lines. (A) PLC/PRF5, HepG2, Hep3B, and Huh7 cell lines were seeded in 24-well plates (3×10^5 cells per well) and allowed to proliferate for 24 hours in complete medium. Then, cells were incubated for a further 72 hours in the presence or not of metformin (1 mM), sorafenib (1 μM), metformin combined with sorafenib, or metformin followed 6 hours later by sorafenib. At the end of the treatment period, cell viability was measured using

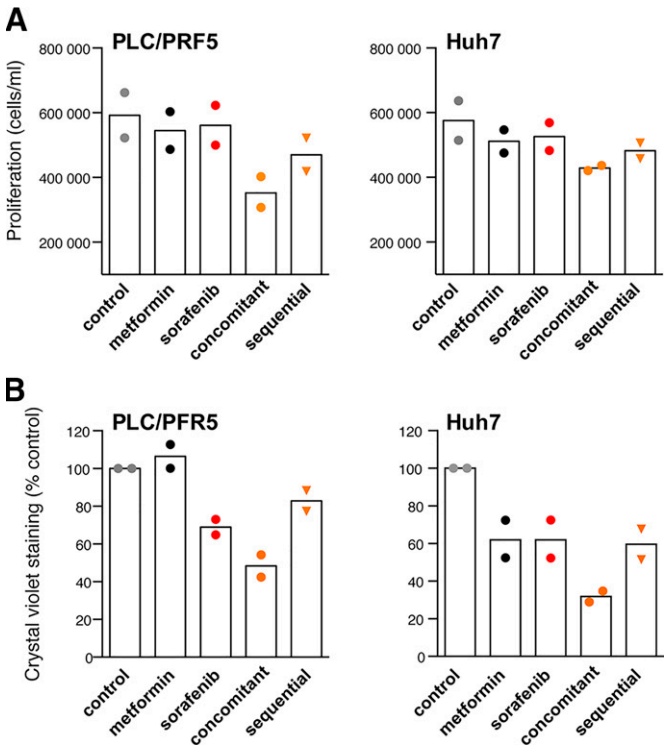

Fig 3. Effects of the concomitant and sequential combinations of metformin and sorafenib on cell proliferation in human HCC cell lines. PLC/PRF5 and Huh7 cell lines were seeded in 24-well plates (3×10^5 cells per well) and allowed to proliferate for 24 hours in complete medium. Then, cells were incubated for a further 72 hours in the presence or not of metformin (1 mM), sorafenib (1 μM), metformin combined with sorafenib, or metformin followed 6 hours later by sorafenib. At the end of the treatment period, cell proliferation was measured by cell counting (A) and staining DNA with 0.1% crystal violet (B). Data are means of two independent experiments performed in eight determinations.

For each significant pathway, the enriched genes were identified, and their recurrence in other pathways was searched as previously described (Hamoudi et al., 2010). The genes detected in more than three different pathways were considered as significant for the drug mechanism of action (Supplemental Table 5). Applying this approach to concomitant drug treatment, 11 members of the olfactory receptors (OR) family (such as *OR10H3* and *OR7G1*) as well as other genes such as *carcinoembryonic antigen-related cell adhesion molecule 1* (*CEACAM1*), *sodium voltage-gated channel alpha subunit 1* (*SCN1A*), and *ADAM metallopeptidase domain 8* (*ADAM8*), among others, were found significantly overexpressed in treated tumors compared with untreated control tumors (*OR10H3*: fold change = 1.38, $P = 0.0228$; *OR11G2*: fold change = 1.29, $P = 0.0175$; *OR13D1*: fold change = 1.33, $P = 0.0347$; *CEACAM1*: fold change = 2.84, $P = 0.0009$; *ADAM8*: fold change = 1.65, $P = 0.017$), and seven members of the olfactory receptors family (such as *OR2AG2* and *OR2T10*) were downregulated (*OR2AG2*: fold change = −1.43, $P = 0.0173$; *OR2T10*: fold change = −1.35, $P = 0.0137$).

In sequential treatment, *protein kinase cAMP-dependent type I regulatory subunit alpha (PRKAR1A)*, *signal transducer and activator of transcription 3 (STAT3)*, *STAT5B*, *insulin-receptor substrate-2 (IRS2)*, *AKT serine/threonine kinase 2 (AKT2)*, and *CEACAM1* were overexpressed in treated tumors (*PRKAR1A*: fold change = 1.68, $P = 0.0254$; *STAT3*: fold change = 1.18, $P = 0.03$; *STAT5B*: fold change = 1.33, $P = 0.0135$; *IRS2*: fold change = 2.01, $P = 0.0212$; *AKT2*: fold change = 1.42, $P = 0.0163$; *CEACAM1*: fold change = 1.71, $P = 0.0304$), and *fibroblast growth factor 2* (*FGF2*) and *C-C motif chemokine ligand 20* (*CCL20*) were downregulated, among others (*FGF2*: fold change = −1.55, $P = 0.02$; *CCL20*: fold change = −1.91, $P = 0.002$).

Comparing the two modes of treatments, genes detected in more than three pathways and upregulated in sequential treatment compared with concomitant treatment include *phosphodiesterase 4D interacting protein* (*PDE4DIP*) (fold change = 1.91, $P = 0.0245$), and downregulated genes include *peptide-YY* (*PYY*) (fold change = −1.55, $P = 0.0036$) and *Wnt family member 1* (*WNT1*) (fold change = −1.24, $P = 0.0389$).

Altogether, these data substantiate the notion that the combination of metformin and sorafenib according to sequential and concomitant regimens leads to qualitatively and quantitatively different signaling pathways in HCC tumors that may account for differential antitumor responses.

Discussion

In the present study, we investigated the underlying mechanisms that may account for the clinical finding that patients receiving both metformin and sorafenib have reduced survival compared with patients receiving sorafenib alone (Gardini et al., 2015; Casadei Gardini et al., 2017; Casadei Schulte et al., 2019). Using a xenograft model of HCC growth, we identified a differential therapeutic response to the bitherapy metformin/sorafenib depending upon the drug administration schedule (concomitant vs. sequential) and provide novel insights into the complex and interactive molecular mechanism of the metformin/sorafenib combination.

Sorafenib has been the gold standard, first-line systemic treatment of advanced HCC since 2007. It provides a modest but significant survival benefit over placebo (Marisi et al., 2018). Sorafenib is a multikinase inhibitor targeting Raf kinase activity, STAT3-dependent signaling, and RTKs such as vascular endothelial growth factor receptor, platelet-derived growth factor receptor-β, and c-KIT (Wilhelm et al., 2008; Tai et al., 2011). These pleiotropic actions confer to sorafenib potential inhibitory effects on tumor cell proliferation and neovascularization.

Because of its great potency to reduce liver glucose production, its relatively low cost, and its safety profile, even in the case of cirrhosis (Bhat et al., 2014; Zhang et al., 2014), metformin is the first medication prescribed to patients with T2D. Several studies have also reported a preventive role of

the MTT assay. Data are means ± S.D. of three independent experiments performed in eight determinations. P values were determined using one-way ANOVA relative to the concomitant condition. P values for other multiple comparisons are presented in Supplemental Table 1. (B) Similar experiments were performed in PLC/PRF5 cells treated with different concentrations of metformin (0, 0.5, 1, 23 mM) in combination with sorafenib (0, 1, 2 μM). Data are means of two independent experiments performed in eight determinations. CTRL, control; metf, metformin; sora, sorafenib.

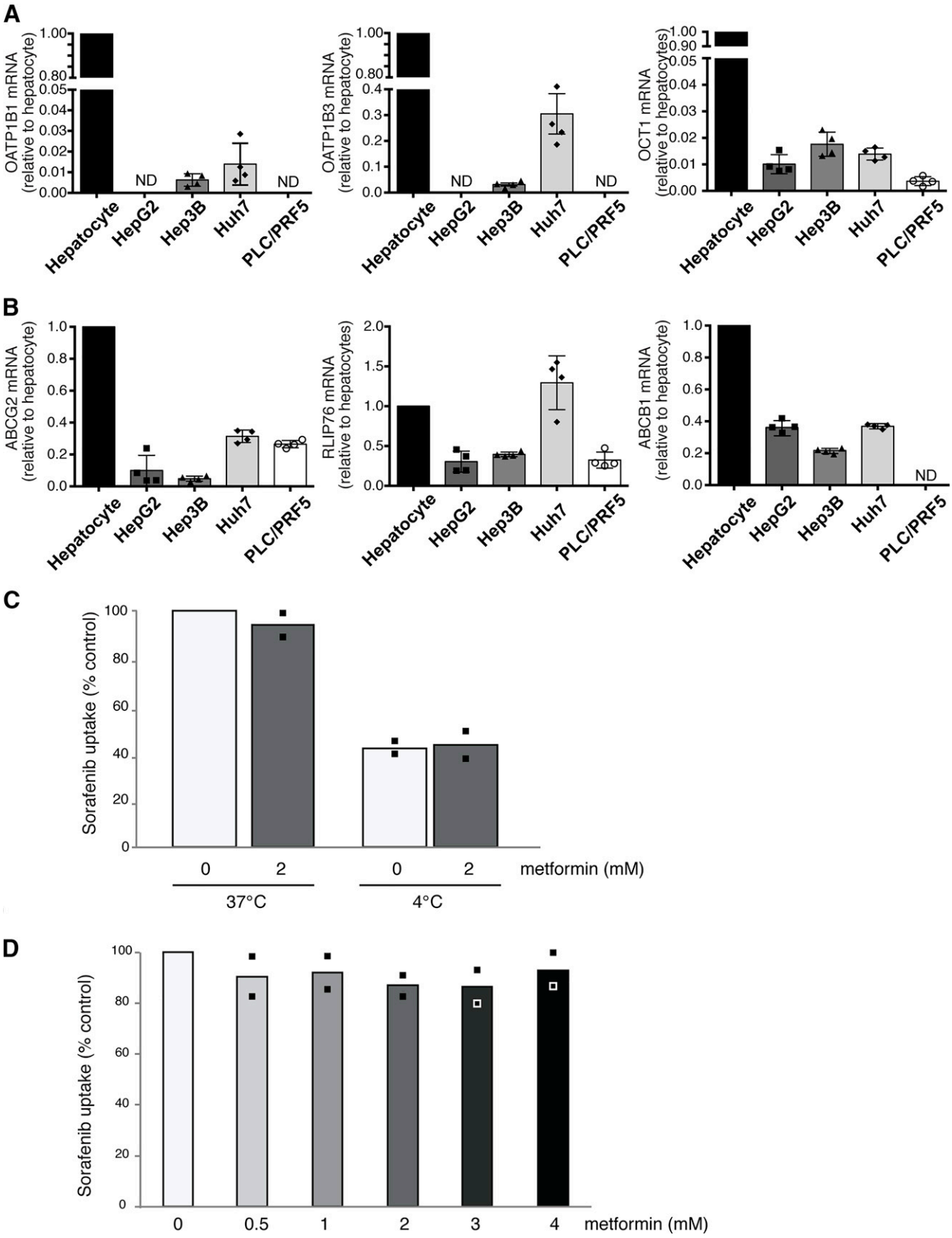

Fig 4. Effects of metformin on the expression of efflux/influx transporters and sorafenib disposal in HCC cell lines. (A and B) Total RNA was extracted from human hepatocytes in primary culture and HCC cell lines, and quantitative measurements of transcripts coding for influx and efflux transporters were performed by real-time polymerase chain reaction. Values are means ± S.D. of four independent experiments. (C and D) Uptake of [^{3}H]sorafenib over 10 minutes in Huh7 cells pretreated for 6 hours in the presence of metformin (0, 0.5, 1, 2, 3–4 mM) at 37°C or 4°C. Data are means of two independent experiments performed in triplicate.

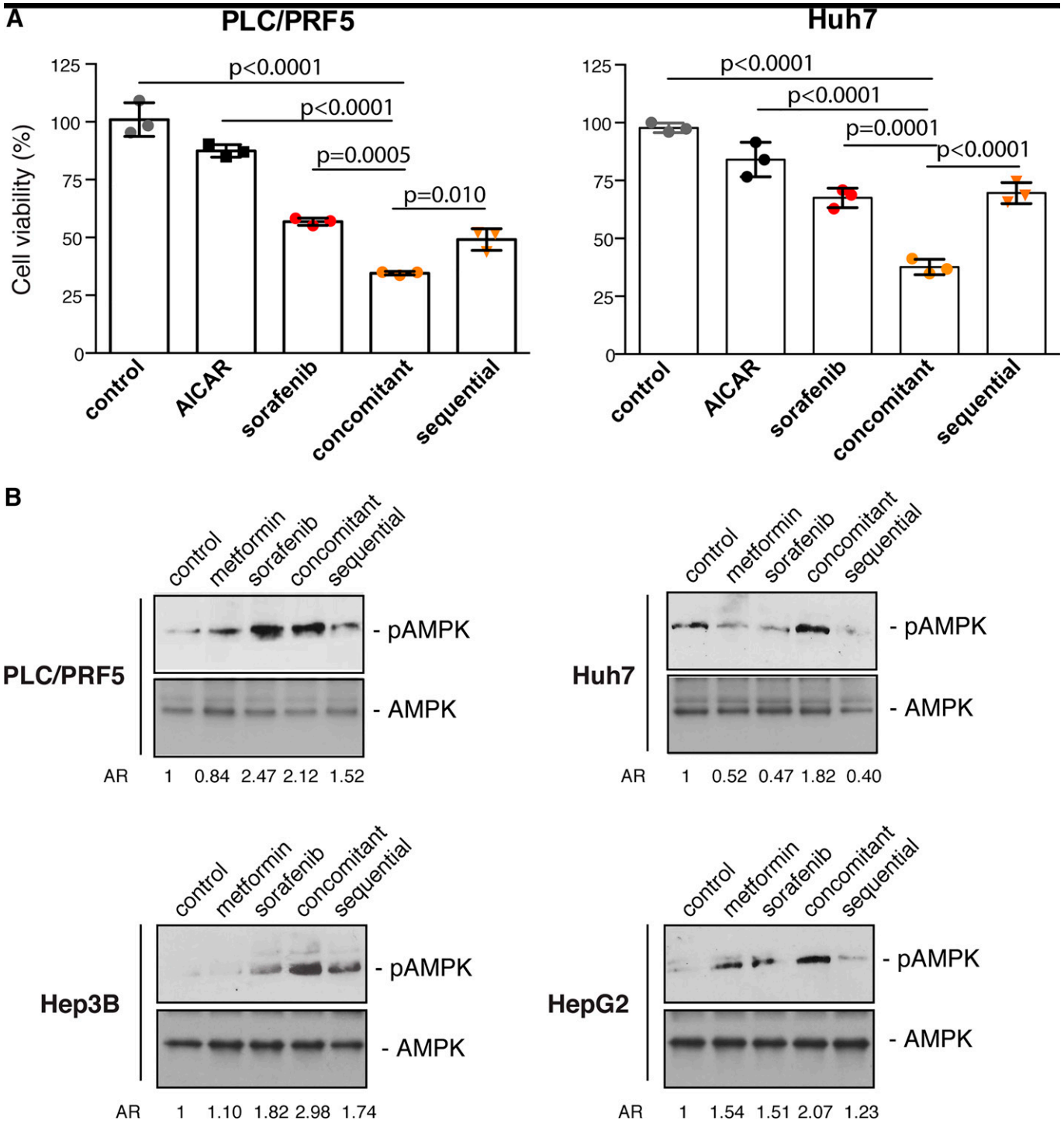

Fig 5. Effects of the concomitant and sequential combinations of metformin and sorafenib on the stimulation of AMPK phosphorylation in human HCC cell lines. (A) PLC/PRF5 and Huh7 cell lines were seeded in 24-well plates (3×10^5 cells per well) and allowed to proliferate for 24 hours in complete medium. Then, cells were incubated for a further 72 hours in the presence or not of AICAR (0.5 mM), sorafenib (1 μM), AICAR combined with sorafenib, or AICAR followed 6 hours later by sorafenib. At the end of the treatment period, cell viability was measured using the MTT assay. Data are means ± S.D. of three independent experiments performed in eight determinations. *P* values were determined using one-way ANOVA relative to the concomitant condition. *P* values for other multiple comparisons are presented in Supplemental Table 1. (B) Whole-cell lysates were analyzed by Western blotting for phosphorylated and total levels of AMPK. Blots are representative of two independent experiments. Values depict the relative pAMPK/AMPK activation ratio (AR) evaluated by scanning densitometry from the two independent experiments.

metformin on HCC development among patients with diabetes (Zhou et al., 2016; Cunha et al., 2020). This is thought to be related to the glucose-lowering and insulin-sensitizing effects of metformin, which might reduce the proliferation rate of premalignant hepatic lesions that thrive in a high-glucose and/or high-insulin environment. In addition, direct

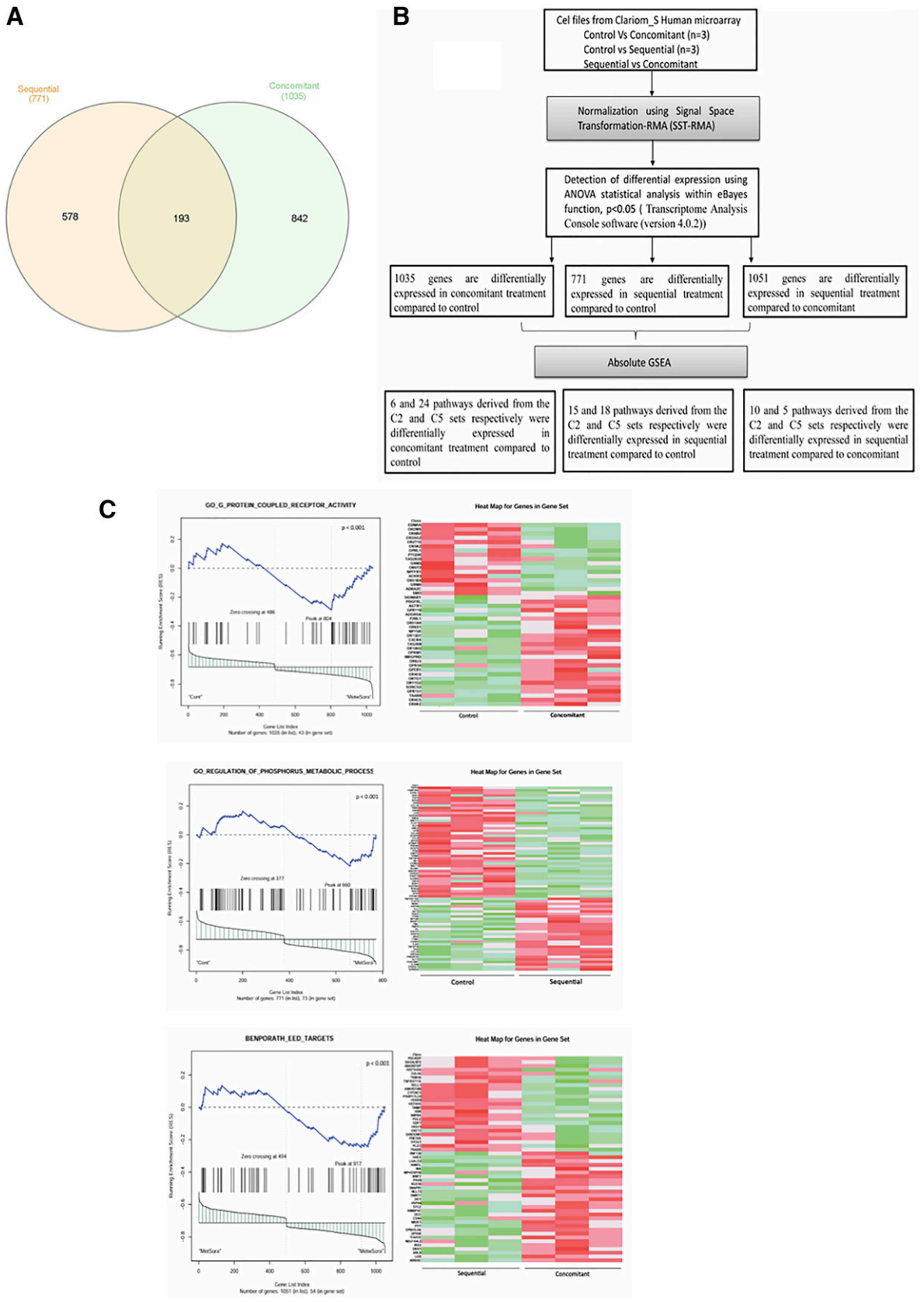

Fig 6. Examples of signatures differentially modulated in xenografted tumors treated with concomitant and sequential metformin/sorafenib administration in comparison with control tumors. (A) Venn diagram showing the numbers of genes differentially expressed between untreated tumors ($n = 3$) and tumors obtained after sequential ($n = 3$) or concomitant ($n = 3$) administration. In total, 1035 genes were identified to be differentially expressed between control and concomitant treatments, 771 genes between control and sequential treatments, and 1051 genes between sequential ($n = 3$) and concomitant treatments. Among these differentially expressed genes, 193 genes were commonly altered by both types of treatments, 842 genes were altered by the concomitant treatment only, and 578 genes by the sequential treatment. (B) Flowchart

antitumor effects of metformin have been reported in vitro in HCC cells (Miyoshi et al., 2014; Tsai et al., 2017; Hu et al., 2019).

Recent observational clinical studies have cast doubt on the benefits for patients with HCC and diabetes to be treated simultaneously with sorafenib and metformin. Indeed, it has been reported that the use of sorafenib and metformin in patients with advanced HCC was associated with a poorer prognosis compared with the use of sorafenib alone (Casadei Gardini et al., 2015, 2017; Schulte et al., 2019). These results were rather unexpected, as preclinical experimental data were encouraging, showing that the concomitant administration of metformin to sorafenib was more efficient than drugs alone to inhibit HCC tumor growth as well metastatic dissemination in immunodeficient mice bearing xenografts of human HCC cells (Guo et al., 2016; You et al., 2016; Ling et al., 2017). However, one limitation of these studies is that metformin was used at a high concentration (>200 mg/kg per day) generally unachievable in patients with diabetes.

Therefore, we conducted the present study to re-evaluate the antitumor potential of the combination metformin/sorafenib, taking into account not only the dose of metformin used but also the drug administration regimen. In contrast to the results reported with high doses of metformin (Chen et al., 2013; Saito et al., 2013; Zheng et al., 2013; Cauchy et al., 2017), we observed that a low dose of metformin (50 mg/kg per day) was unable to inhibit the growth of established tumors in an HCC xenograft model. In this model, the coadministration of sorafenib with a low dose of metformin induced a significant reduction in tumor volume and weight compared with control but was not significantly more effective than sorafenib monotherapy. Taken together, these data suggest that the antitumor effect of metformin cannot be achieved in vivo at a clinically relevant dose.

Intriguingly, the sequential administration of metformin 6 hours prior to sorafenib significantly impaired the anticancer effect of sorafenib on tumor growth in the HCC xenograft model. These observations were reproduced in vitro using a panel of four human HCC cell lines known to be genetically and phenotypically different (Caruso et al., 2019), which supports the relevance of our findings. Cell pretreatment with metformin impaired sorafenib effects on HCC cell viability and proliferation in vitro. Interestingly, we performed preliminary experiments with sunitinib, which is also a pan-inhibitor of receptor tyrosine kinases. In a similar way to what was observed with sorafenib, we found that the sequential treatment with metformin was less effective than the concomitant treatment to decrease cell viability in the PLC/PRF5 cell line (Supplemental Fig. 1), suggesting that metformin may more generally interfere with this class of anticancer drugs.

Prior administration of metformin impacted neither the plasma concentrations of sorafenib 2 and 6 hours after its administration nor the intracellular bioavailability of sorafenib in HCC cells in vitro. Karbownik et al. (2020) recently showed that the concomitant administration of metformin (100 mg/kg) increases the clearance of sorafenib (100 mg/kg) in rats, which results in a lower sorafenib half-life (16.3 ± 3.7 vs. 21.9 ± 7.8 hours, $P = 0.0372$). This result was obtained from complete sorafenib pharmacokinetics including sampling points up to 96 hours. The difference was particularly significant during the terminal elimination phase (i.e., 24 hours after the administration). Therefore, our limited sampling strategy (two sampling points at 2 and 6 hours after administration) is a limiting factor to draw any conclusion about the pharmacokinetic interaction between metformin and sorafenib, and this point deserves further characterization. According to the results of Karbownik et al. (2020), we should have expected a lower total exposure to sorafenib in our murine model cotreated with metformin. However, coadministration of sorafenib plus metformin was associated with a greater decrease in tumor volume compared with sequential therapy in our model, which suggests that the differential effects between the two regimens may be the result of pharmacodynamic rather than pharmacokinetic interactions.

The sequential use of metformin and sorafenib led to a poorer activation of AMPK in HCC cell lines than did the concomitant treatment. Metformin alone has been reported to exert some of its anticancer effects in HCC cells through the activation of AMPK and the subsequent inhibition of mTOR signaling (Zheng et al., 2013; Cheng et al., 2014). In addition, low levels of AMPK signaling has been associated with HCC cell resistance to sorafenib (Bort et al., 2019). Together with our in vitro findings showing that cell pretreatment with AICAR, another AMPK activator, impaired HCC cell response to sorafenib, these data sustain the hypothesis that the deficit in AMPK signaling as evidenced in HCC cells pretreated with metformin participates in tumor cell resistance to sorafenib.

The microarray analysis performed on RNA extracted from tumor xenografts confirmed that gene expression and cellular pathways are differentially altered by sequential and concomitant treatments with metformin and sorafenib. Of interest, pathways altered by the concomitant treatment mainly involve GPCRs, which may account for its beneficial effect observed in vivo compared with sequential. GPCRs are known to increase intracellular levels of cAMP by activating adenylate cyclase, which may concur with the subsequent stimulation of protein kinase A (PKA), LKB1, and AMPK. In contrast, the sequential regimen rather altered pathways involving RTKs (*IRS2* and *AKT2* overexpression), STAT signaling (*STAT3* and *STAT5B* overexpression), and perturbation of cAMP signaling (*PRKAR1A*), which may account for its

outlining the steps of the bioinformatics approach to identify differentially expressed genes in concomitant and sequential treatments compared with controls. RNA samples were hybridized to Human Clariom S GeneChip. After normalization using Signal Space Transformation-RMA, differential expression was carried out using eBayes function and one-way ANOVA statistical analysis. The analysis was carried out using Transcriptome Analysis Console software. The differentially expressed genes were then subjected to absolute GSEA searching through more than 10,000 different cellular pathways. (C) Examples of signatures differentially modulated in xenografted tumors treated with concomitant and sequential metformin/sorafenib administration in comparison with control tumors. Upper: GSEA of GO_G_PROTEIN_COUPLED_RECEPTOR_ACTIVITY (GO:0007186) in HCC xenografts treated with concomitant combination of metformin and sorafenib in comparison with control group; middle: GSEA of GO_REGULATION_OF_PHOSPHORUS_METABOLIC_PROCESS (GO:0051174) in HCC xenografts treated with sequential combination of metformin followed by sorafenib in comparison with control group; lower: GSEA of BENPORATH_EED_TARGETS (M7617) in HCC xenografts treated with sequential combination of metformin followed by sorafenib in comparison with concomitant treatment.

lack of efficacy compared with the concomitant administration. *PRKAR1A* codes for the type 1α regulatory subunit of PKA and its overexpression have been reported in different cancer cell types. Downregulation of *PRKAR1A* in cancer cells with small interfering RNA was shown to activate PKA through release of the catalytic subunit from the holoenzyme (Nadella et al., 2008).

The transcriptomic analysis also showed that both regimens induce expression of genes associated with therapeutic resistance and tumor progression. Regarding the sequential treatment, microarray analysis identified *FGF2* and *CCL20* as downregulated after sequential treatment. *FGF2* downregulation could reduce elimination of HCC cells by natural killer–mediated innate immunity as previously reported (Tsunematsu et al., 2012) and thus contribute to reduced treatment efficacy. As upregulation of *CCL20* was previously reported in sorafenib responders versus nonresponders (Covell, 2017), its downregulation is probably a marker of inefficacy of sequential combination. *CEACAM1* was upregulated in combinatory and sequential treatments, and its upregulation has been associated with HCC invasion, progression, and recurrence (Kiriyama et al., 2014; Yoshikawa et al., 2017; Park et al., 2020). *ADAM8* was overexpressed in concomitant treatment versus control. High expression of *ADAM8* was previously found to correlate with progression and poor prognosis in patients with HCC (Jiang et al., 2012; Zhang et al., 2013). These data suggest that despite its ability to target GPCR and AMPK signaling, the combination metformin/sorafenib may also induce adverse signaling pathways that ultimately contribute to drug resistance and treatment failure, raising doubt about its benefit in the treatment of HCC.

In conclusion, our study provides important information on the molecular mechanisms of action of the metformin/sorafenib combination and suggests a pharmacodynamics drug interaction between the two molecules, leading to a loss of antitumor activity. Our data call into question the benefit of parallel use of the two drugs in patients suffering from both advanced HCC and diabetes, as this interaction could ultimately compromise patient survival.

Acknowledgments

The authors are greatly indebted to Corina Buta and Alkaly Gassama for their technical assistance. We thank Sébastien Jacques, Angéline Duché, and Franck Letourneur from the platform GENOM'IC (Cochin Institute, INSERM U1016, Paris) for microarray experiments and Tatiana Ledent and the staff of the animal facility of the Saint-Antoine Research Center (INSERM UMR_S938) for animal care and welfare.

Authorship Contributions

Participated in Research design: Harati, Vandamme, Desbois-Mouthon.

Conducted experiments: Harati, Vandamme, Desbois-Mouthon.

Contributed new reagents or analytic tools: Blanchet, Bardin, Hamoudi.

Performed data analysis: Harati, Vandamme, Hamoudi, Desbois-Mouthon.

Wrote or contributed to the writing of manuscript: Harati, Blanchet, Praz, Hamoudi, Desbois-Mouthon.

References

Agarwal S and Elmquist WF (2012) Insight into the cooperation of P-glycoprotein (ABCB1) and breast cancer resistance protein (ABCG2) at the blood-brain barrier: a case study examining sorafenib efflux clearance. *Mol Pharm* **9**:678–684.

Agarwal S, Sane R, Ohlfest JR, and Elmquist WF (2011) The role of the breast cancer resistance protein (ABCG2) in the distribution of sorafenib to the brain. *J Pharmacol Exp Ther* **336**:223–233.

Anstee QM, Reeves HL, Kotsiliti E, Govaere O, and Heikenwalder M (2019) From NASH to HCC: current concepts and future challenges. *Nat Rev Gastroenterol Hepatol* **16**:411–428.

Aoudjehane L, Boelle PY, Bisch G, Delelo R, Paye F, Scatton O, Housset C, Becquart J, Calmus Y, and Conti F (2016) Development of an in vitro model to test antifibrotic drugs on primary human liver myofibroblasts. *Lab Invest* **96**:672–679.

Ashburner M, Ball CA, Blake JA, Botstein D, Butler H, Cherry JM, Davis AP, Dolinski K, Dwight SS, Eppig JT, et al.; The Gene Ontology Consortium (2000) Gene ontology: tool for the unification of biology. *Nat Genet* **25**:25–29.

Bardin C, Nobecourt E, Larger E, Chast F, Treluyer JM, and Urien S (2012) Population pharmacokinetics of metformin in obese and non-obese patients with type 2 diabetes mellitus. *Eur J Clin Pharmacol* **68**:961–968.

Bhat M, Chaiteerakij R, Harmsen WS, Schleck CD, Yang JD, Giama NH, Therneau TM, Gores GJ, and Roberts LR (2014) Metformin does not improve survival in patients with hepatocellular carcinoma. *World J Gastroenterol* **20**:15750–15755.

Blanchet B, Billemont B, Cramard J, Benichou AS, Chhun S, Harcouet L, Ropert S, Dauphin A, Goldwasser F, and Tod M (2009) Validation of an HPLC-UV method for sorafenib determination in human plasma and application to cancer patients in routine clinical practice. *J Pharm Biomed Anal* **49**:1109–1114.

Blivet-Van Eggelpoël MJ, Chettouh H, Fartoux L, Aoudjehane L, Barbu V, Rey C, Priam S, Housset C, Rosmorduc O, and Desbois-Mouthon C (2012) Epidermal growth factor receptor and HER-3 restrict cell response to sorafenib in hepatocellular carcinoma cells. *J Hepatol* **57**:108–115.

Bort A, Sánchez BG, Mateos-Gómez PA, Vara-Ciruelos D, Rodríguez-Henche N, and Díaz-Laviada I (2019) Targeting AMP-activated kinase impacts hepatocellular cancer stem cells induced by long-term treatment with sorafenib. *Mol Oncol* **13**:1311–1331.

Cai H, Everett RS, and Thakker DR (2019) Efficacious dose of metformin for breast cancer therapy is determined by cation transporter expression in tumours. *Br J Pharmacol* **176**:2724–2735.

Caruso S, Calatayud AL, Pilet J, La Bella T, Rekik S, Imbeaud S, Letouzé E, Meunier L, Bayard Q, Rohr-Udilova N, et al. (2019) Analysis of liver cancer cell lines identifies agents with likely efficacy against hepatocellular carcinoma and markers of Response. *Gastroenterology* **157**:760–776.

Casadei Gardini A, Faloppi L, De Matteis S, Foschi FG, Silvestris N, Tovoli F, Palmieri V, Marisi G, Brunetti O, Vespasiani-Gentilucci U, et al. (2017) Metformin and insulin impact on clinical outcome in patients with advanced hepatocellular carcinoma receiving sorafenib: Validation study and biological rationale. *Eur J Cancer* **86**:106–114.

Casadei Gardini A, Marisi G, Scarpi E, Scartozzi M, Faloppi L, Silvestris N, Masi G, Vivaldi C, Brunetti O, Tamberi S, et al. (2015) Effects of metformin on clinical outcome in diabetic patients with advanced HCC receiving sorafenib. *Expert Opin Pharmacother* **16**:2719–2725.

Cauchy F, Mebarki M, Leporq B, Laouirem S, Albuquerque M, Lambert S, Bourgoin P, Soubrane O, Van Beers BE, Faivre S, et al. (2017) Strong antineoplastic effects of metformin in preclinical models of liver carcinogenesis. *Clin Sci (Lond)* **131**:27–36.

Chen HP, Shieh JJ, Chang CC, Chen TT, Lin JT, Wu MS, Lin JH, and Wu CY (2013) Metformin decreases hepatocellular carcinoma risk in a dose-dependent manner: population-based and in vitro studies. *Gut* **62**:606–615.

Cheng J, Huang T, Li Y, Guo Y, Zhu Y, Wang Q, Tan X, Chen W, Zhang Y, Cheng W et al. (2014) AMP-activated protein kinase suppresses the in vitro and in vivo proliferation of hepatocellular carcinoma. *PLoS One* **9**:e93256.

Covell DG (2017) A data mining approach for identifying pathway-gene biomarkers for predicting clinical outcome: a case study of erlotinib and sorafenib. *PLoS One* **12**:e0181991.

Croft D, O'Kelly G, Wu G, Haw R, Gillespie M, Matthews L, Caudy M, Garapati P, Gopinath G, Jassal B, et al. (2011) Reactome: a database of reactions, pathways and biological processes. *Nucleic Acids Res* **39**:D691–D697.

Cunha V, Cotrim HP, Rocha R, Carvalho K, and Lins-Kusterer L (2020) Metformin in the prevention of hepatocellular carcinoma in diabetic patients: a systematic review. *Ann Hepatol* **19**:232–237.

Desbois-Mouthon C, Baron A, Blivet-Van Eggelpoël MJ, Fartoux L, Venot C, Bladt F, Housset C, and Rosmorduc O (2009) Insulin-like growth factor-1 receptor inhibition induces a resistance mechanism via the epidermal growth factor receptor/HER3/AKT signaling pathway: rational basis for cotargeting insulin-like growth factor-1 receptor and epidermal growth factor receptor in hepatocellular carcinoma. *Clin Cancer Res* **15**:5445–5456.

Dowling RJ, Lam S, Bassi C, Mouaaz S, Aman A, Kiyota T, Al-Awar R, Goodwin PJ, and Stambolic V (2016) Metformin pharmacokinetics in mouse tumors: implications for human therapy. *Cell Metab* **23**:567–568.

Edginton AN, Zimmerman EI, Vasilyeva A, Baker SD, and Panetta JC (2016) Sorafenib metabolism, transport, and enterohepatic recycling: physiologically based modeling and simulation in mice. *Cancer Chemother Pharmacol* **77**:1039–1052.

Ferlay J, Colombet M, Soerjomataram I, Mathers C, Parkin DM, Piñeros M, Znaor A, and Bray F (2019) Estimating the global cancer incidence and mortality in 2018: GLOBOCAN sources and methods. *Int J Cancer* **144**:1941–1953.

Foretz M, Hébrard S, Leclerc J, Zarrinpashneh E, Soty M, Mithieux G, Sakamoto K, Andreelli F, and Viollet B (2010) Metformin inhibits hepatic gluconeogenesis in mice independently of the LKB1/AMPK pathway via a decrease in hepatic energy state. *J Clin Invest* **120**:2355–2369.

Goumard C, Desbois-Mouthon C, Wendum D, Calmel C, Merabtene F, Scatton O, and Praz F (2017) Low levels of microsatellite instability at simple repeated sequences commonly occur in human hepatocellular carcinoma. *Cancer Genomics Proteomics* **14**:329–339.

Groenendijk FH, Mellema WW, van der Burg E, Schut E, Hauptmann M, Horlings HM, Willems SM, van den Heuvel MM, Jonkers J, Smit EF, et al. (2015) Sorafenib synergizes with metformin in NSCLC through AMPK pathway activation. *Int J Cancer* **136**:1434–1444.

Guo Z, Cao M, You A, Gao J, Zhou H, Li H, Cui Y, Fang F, Zhang W, Song T, et al. (2016) Metformin inhibits the prometastatic effect of sorafenib in hepatocellular carcinoma by upregulating the expression of TIP30. *Cancer Sci* **107**:507–513.

Hamoudi RA, Appert A, Ye H, Ruskone-Fourmestraux A, Streubel B, Chott A, Raderer M, Gong L, Wlodarska I, De Wolf-Peeters C, et al. (2010) Differential expression of NF-kappaB target genes in MALT lymphoma with and without chromosome translocation: insights into molecular mechanism. *Leukemia* **24**:1487–1497.

Haouala A, Rumpold H, Untergasser G, Buclin T, Ris HB, Widmer N, and Decosterd LA (2010) siRNA-mediated knock-down of P-glycoprotein expression reveals distinct cellular disposition of anticancer tyrosine kinases inhibitors. *Drug Metab Lett* **4**:114–119.

Heishi M, Ichihara J, Teramoto R, Itakura Y, Hayashi K, Ishikawa H, Gomi H, Sakai J, Kanaoka M, Taiji M, et al. (2006) Global gene expression analysis in liver of obese diabetic db/db mice treated with metformin. *Diabetologia* **49**:1647–1655.

Herraez E, Lozano E, Macias RI, Vaquero J, Bujanda L, Banales JM, Marin JJ, and Briz O (2013) Expression of SLC22A1 variants may affect the response of hepatocellular carcinoma and cholangiocarcinoma to sorafenib. *Hepatology* **58**:1065–1073.

Hou M, Venier N, Sugar L, Musquera M, Pollak M, Kiss A, Fleshner N, Klotz L, and Venkateswaran V (2010) Protective effect of metformin in CD1 mice placed on a high carbohydrate-high fat diet. *Biochem Biophys Res Commun* **397**:537–542.

Hu L, Zeng Z, Xia Q, Liu Z, Feng X, Chen J, Huang M, Chen L, Fang Z, Liu Q, et al. (2019) Metformin attenuates hepatoma cell proliferation by decreasing glycolytic flux through the HIF-1α/PFKFB3/PFK1 pathway. *Life Sci* **239**:116966.

Hu S, Chen Z, Franke R, Orwick S, Zhao M, Rudek MA, Sparreboom A, and Baker SD (2009) Interaction of the multikinase inhibitors sorafenib and sunitinib with solute carriers and ATP-binding cassette transporters. *Clin Cancer Res* **15**:6062–6069.

Huang WC, Hsieh YL, Hung CM, Chien PH, Chien YF, Chen LC, Tu CY, Chen CH, Hsu SC, Lin YM, et al. (2013) BCRP/ABCG2 inhibition sensitizes hepatocellular carcinoma cells to sorafenib. *PLoS One* **8**:e83627.

Irizarry RA, Bolstad BM, Collin F, Cope LM, Hobbs B, and Speed TP (2003) Summaries of affymetrix GeneChip probe level data. *Nucleic Acids Res* **31**:e15.

Jiang C, Zhang Y, Yu HF, Yu XT, Zhou SJ, and Tan YF (2012) Expression of ADAM8 and its clinical values in diagnosis and prognosis of hepatocellular carcinoma. *Tumour Biol* **33**:2167–2172.

Kanehisa M and Goto S (2000) KEGG: kyoto encyclopedia of genes and genomes. *Nucleic Acids Res* **28**:27–30.

Karbownik A, Szkutnik-Fiedler D, Czyrski A, Kostewicz N, Kaczmarska P, Bekier M, Stanisławiak-Rudowicz J, Karaźniewicz-Łada M, Wolc A, Główka F, et al. (2020) Pharmacokinetic interaction between sorafenib and atorvastatin, and sorafenib and metformin in rats. *Pharmaceutics* **12**:600.

Kiriyama S, Yokoyama S, Ueno M, Hayami S, Ieda J, Yamamoto N, Yamaguchi S, Mitani Y, Nakamura Y, Tani M. et al. (2014) CEACAM1 long cytoplasmic domain isoform is associated with invasion and recurrence of hepatocellular carcinoma. *Ann Surg Oncol* **21** (Suppl 4):S505–S514.

Lalau JD, Lemaire-Hurtel AS, and Lacroix C (2011) Establishment of a database of metformin plasma concentrations and erythrocyte levels in normal and emergency situations. *Clin Drug Investig* **31**:435–438.

Ling S, Song L, Fan N, Feng T, Liu L, Yang X, Wang M, Li Y, Tian Y, Zhao F, et al. (2017) Combination of metformin and sorafenib suppresses proliferation and induces autophagy of hepatocellular carcinoma via targeting the mTOR pathway. *Int J Oncol* **50**:297–309.

Marisi G, Cucchetti A, Ulivi P, Canale M, Cabibbo G, Solaini L, Foschi FG, De Matteis S, Ercolani G, Valgiusti M, et al. (2018) Ten years of sorafenib in hepatocellular carcinoma: are there any predictive and/or prognostic markers? *World J Gastroenterol* **24**:4152–4163.

Miyoshi H, Kato K, Iwama H, Maeda E, Sakamoto T, Fujita K, Toyota Y, Tani J, Nomura T, Mimura S, et al. (2014) Effect of the anti-diabetic drug metformin in hepatocellular carcinoma in vitro and in vivo. *Int J Oncol* **45**:322–332.

Nadella KS, Jones GN, Trimboli A, Stratakis CA, Leone G, and Kirschner LS (2008) Targeted deletion of Prkar1a reveals a role for protein kinase A in mesenchymal-to-epithelial transition. *Cancer Res* **68**:2671–2677.

Park DJ, Sung PS, Kim JH, Lee GW, Jang JW, Jung ES, Bae SH, Choi JY, and Yoon SK (2020) EpCAM-high liver cancer stem cells resist natural killer cell-mediated cytotoxicity by upregulating CEACAM1. *J Immunother Cancer* **8**:e000301.

Poller B, Wagenaar E, Tang SC, and Schinkel AH (2011) Double-transduced MDCKII cells to study human P-glycoprotein (ABCB1) and breast cancer resistance protein (ABCG2) interplay in drug transport across the blood-brain barrier. *Mol Pharm* **8**:571–582.

Saito T, Chiba T, Yuki K, Zen Y, Oshima M, Koide S, Motoyama T, Ogasawara S, Suzuki E, Ooka Y, et al. (2013) Metformin, a diabetes drug, eliminates tumor-initiating hepatocellular carcinoma cells. *PLoS One* **8**:e70010.

Schulte L, Scheiner B, Voigtländer T, Koch S, Schweitzer N, Marhenke S, Ivanyi P, Manns MP, Rodt T, Hinrichs JB, et al. (2019) Treatment with metformin is associated with a prolonged survival in patients with hepatocellular carcinoma. *Liver Int* **39**:714–726.

Singhal SS, Sehrawat A, Sahu M, Singhal P, Vatsyayan R, Rao Lelsani PC, Yadav S, and Awasthi S (2010) Rlip76 transports sunitinib and sorafenib and mediates drug resistance in kidney cancer. *Int J Cancer* **126**:1327–1338.

Swift B, Nebot N, Lee JK, Han T, Proctor WR, Thakker DR, Lang D, Radtke M, Gnoth MJ, and Brouwer KL (2013) Sorafenib hepatobiliary disposition: mechanisms of hepatic uptake and disposition of generated metabolites. *Drug Metab Dispos* **41**:1179–1186.

Tai WT, Cheng AL, Shiau CW, Huang HP, Huang JW, Chen PJ, and Chen KF (2011) Signal transducer and activator of transcription 3 is a major kinase-independent target of sorafenib in hepatocellular carcinoma. *J Hepatol* **55**:1041–1048.

Tang SC, de Vries N, Sparidans RW, Wagenaar E, Beijnen JH, and Schinkel AH (2013) Impact of P-glycoprotein (ABCB1) and breast cancer resistance protein (ABCG2) gene dosage on plasma pharmacokinetics and brain accumulation of dasatinib, sorafenib, and sunitinib. *J Pharmacol Exp Ther* **346**:486–494.

Tsai HH, Lai HY, Chen YC, Li CF, Huang HS, Liu HS, Tsai YS, and Wang JM (2017) Metformin promotes apoptosis in hepatocellular carcinoma through the CEBPD-induced autophagy pathway. *Oncotarget* **8**:13832–13845.

Tsunematsu H, Tatsumi T, Kohga K, Yamamoto M, Aketa H, Miyagi T, Hosui A, Hiramatsu N, Kanto T, Hayashi N, et al. (2012) Fibroblast growth factor-2 enhances NK sensitivity of hepatocellular carcinoma cells. *Int J Cancer* **130**:356–364.

Wilhelm SM, Adnane L, Newell P, Villanueva A, Llovet JM, and Lynch M (2008) Preclinical overview of sorafenib, a multikinase inhibitor that targets both Raf and VEGF and PDGF receptor tyrosine kinase signaling. *Mol Cancer Ther* **7**:3129–3140.

Yarchoan M, Agarwal P, Villanueva A, Rao S, Dawson LA, Llovet JM, Finn RS, Groopman JD, El-Serag HB, Monga SP, et al. (2019) Recent developments and therapeutic strategies against hepatocellular carcinoma. *Cancer Res* **79**:4326–4330.

Yoshikawa M, Morine Y, Ikemoto T, Imura S, Higashijima J, Iwahashi S, Saito YU, Takasu C, Yamada S, Ishikawa D, et al. (2017) Elevated preoperative serum CEA level is associated with poor prognosis in patients with hepatocellular carcinoma through the epithelial-mesenchymal transition. *Anticancer Res* **37**:1169–1175.

You A, Cao M, Guo Z, Zuo B, Gao J, Zhou H, Li H, Cui Y, Fang F, Zhang W, et al. (2016) Metformin sensitizes sorafenib to inhibit postoperative recurrence and metastasis of hepatocellular carcinoma in orthotopic mouse models. *J Hematol Oncol* **9**:20.

Younossi ZM, Golabi P, de Avila L, Paik JM, Srishord M, Fukui N, Qiu Y, Burns L, Afendy A, and Nader F, (2019) The global epidemiology of NAFLD and NASH in patients with type 2 diabetes: a systematic review and meta-analysis. *J Hepatol* **71**:793–801.

Zhang X, Harmsen WS, Mettler TA, Kim WR, Roberts RO, Therneau TM, Roberts LR, and Chaiteerakij R (2014) Continuation of metformin use after a diagnosis of cirrhosis significantly improves survival of patients with diabetes. *Hepatology* **60**:2008–2016.

Zhang Y, Zha TZ, Hu BS, Jiang C, Ge ZJ, Zhang K, and Tan YF (2013) High expression of ADAM8 correlates with poor prognosis in hepatocellular carcinoma. *Surgeon* **11**:67–71.

Zheng L, Yang W, Wu F, Wang C, Yu L, Tang L, Qiu B, Li Y, Guo L, Wu M, et al. (2013) Prognostic significance of AMPK activation and therapeutic effects of metformin in hepatocellular carcinoma. *Clin Cancer Res* **19**:5372–5380.

Zhou YY, Zhu GQ, Liu T, Zheng JN, Cheng Z, Zou TT, Braddock M, Fu SW, and Zheng MH (2016) Systematic review with network meta-analysis: antidiabetic medication and risk of hepatocellular carcinoma. *Sci Rep* **6**:33743.

Zimmerman EI, Hu S, Roberts JL, Gibson AA, Orwick SJ, Li L, Sparreboom A, and Baker SD (2013) Contribution of OATP1B1 and OATP1B3 to the disposition of sorafenib and sorafenib-glucuronide. *Clin Cancer Res* **19**:1458–1466.

Address correspondence to: Dr. Christèle Desbois-Mouthon, Centre de Recherche des Cordeliers, INSERM UMR_S1138, 15 rue de l'école de médecine, 75006 Paris, France; E-mail: christele.desbois-mouthon@inserm.fr